# Supporting Information

# Corona-Dependent Enhanced Fluorescence Response of Defects-Induced Single-Walled Carbon Nanotubes to Organophosphate

*Gali Etus,*[a] *Srestha Basu,* [b,c,d] *Adi Hendler-Neumark,* [b] *and Gili Bisker* [*b,e,f,g,h,i]

[a] School of Electrical Engineering, Faculty of Engineering, Tel Aviv University, Tel Aviv 6997801, Israel
[b] School of Biomedical Engineering, Faculty of Engineering, Tel Aviv University, Tel Aviv 6997801, Israel
[c] Biophysical Sciences Group, Saha Institute of Nuclear Physics, 1/AF Bidhannagar, Kolkata 700064, India
[d] Chemical Sciences Division, Homi Bhabha National Institute, Mumbai 400094, India
[e] Center for Physics and Chemistry of Living Systems, Tel Aviv University, Tel Aviv 6997801, Israel
[f] Center for Nanoscience and Nanotechnology, Tel Aviv University, Tel Aviv 6997801, Israel
[g] Center for Light-Matter Interaction, Tel Aviv University, Tel Aviv 6997801, Israel
[h] Sagol School of Neuroscience, Tel Aviv University, Tel Aviv 6997801, Israel
[i] The Center for Computational Molecular and Materials Science, Tel Aviv University, Tel Aviv 6997801, Israel

Email: bisker@tauex.tau.ac.il

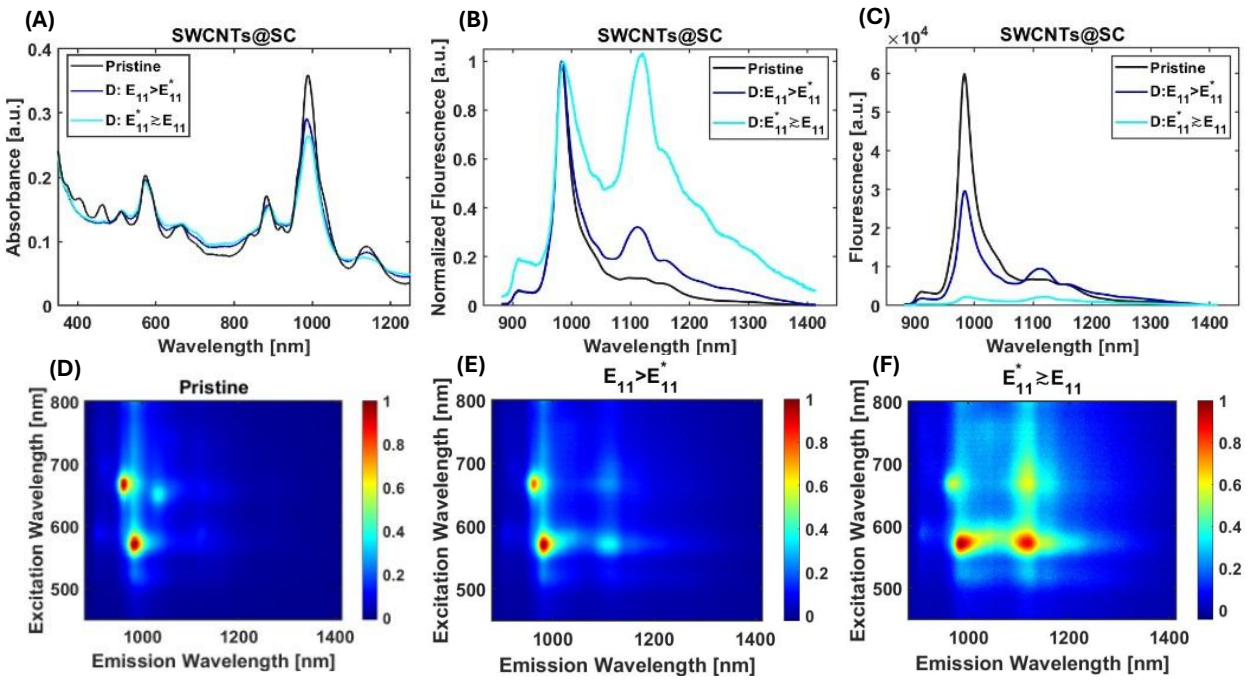


**Figure S1.** Spectroscopic characterization of pristine SWCNTs@SC and D-SWCNTs@SC suspensions. **(A)** UV-vis-NIR absorption of SWCNTs@SC (black curve) and D-SWCNTs@SC treated with NaClO and UV irradiation for 5 min (blue curve) and 15 min (cyan curve). **(B)** Normalized fluorescence spectra of pristine SWCNTs@SC (black curve) and D-SWCNTs@SC with UV exposure for 5 min (blue curve) and 15 min (cyan curve), and **(C)** the un-normalized respective spectra. The 5- and 15-minute exposures resulted in an $E_{11}>E_{11}^*$ and $E_{11}^* \gtrsim E_{11}$ peak ratios, respectively. **(D)** Excitation-emission map of pristine SWCNTs@SC, and **(E)** D-SWCNTs@SC with UV irradiation for 5 min and **(F)** 15 min.

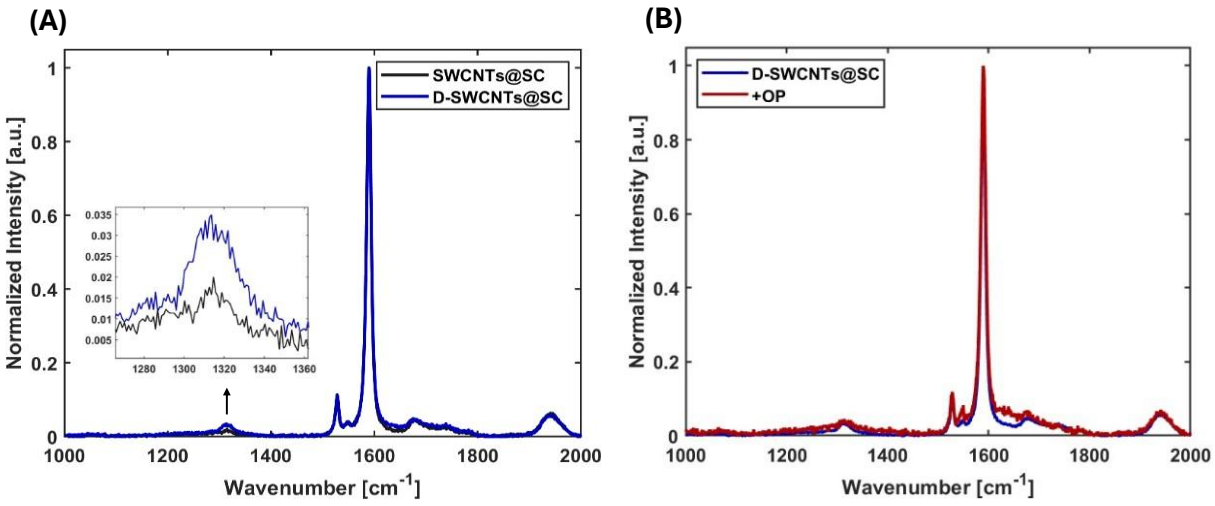


**Figure S2.** Raman spectroscopy. **(A)** Raman spectra of SWCNTs@SC (black) and D-SWCNTs@SC (blue) following 5 min UV irradiation. Inset: A distinct D-band is observed in the D-SWCNTs@SC sample, signifying the successful introduction of oxygen defects. **(B)** Raman spectra comparing D-SWCNTs@SC (blue) and D-SWCNTs@SC after OP treatment (red), showing no apparent difference.

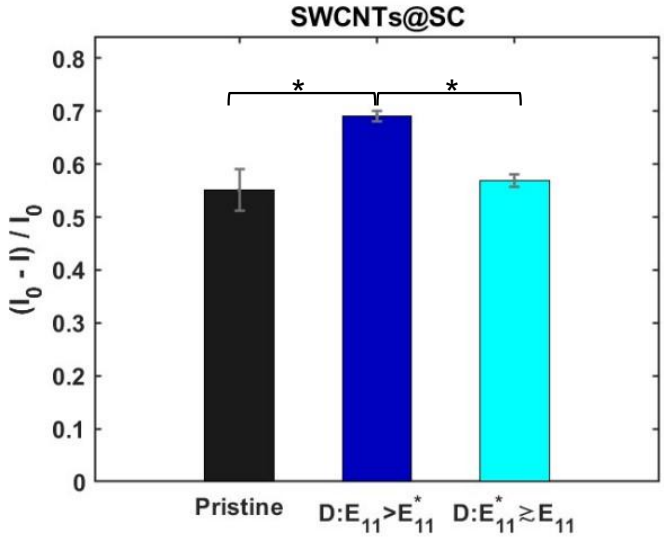


**Figure S3.** Normalized fluorescence response upon OP addition, calculated as $(I_0 - I)/I_0$, for pristine SWCNTs@SC (black bar) and D-SWCNTs@SC prepared with 5-minute UV exposure (blue bar) and 15-minute UV exposure (cyan bar). Here, $I_0$ represents the $E_{11}$ fluorescence peak intensity prior to OP addition, while $I$ corresponds to the $E_{11}$ intensity following OP addition. Error bars represent the standard deviation from three independent measurements. Statistical comparisons were performed using unpaired two-tailed t-tests. Asterisks (*) denote statistically significant differences with $p < 0.05$.

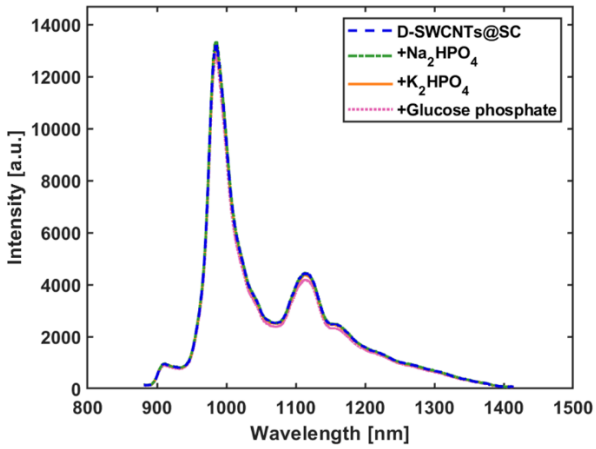


**Figure S4.** Selectivity test of D-SWCNTs@SC. Fluorescence spectra of D-SWCNTs@SC before and after the addition of representative inorganic phosphates and glucose phosphate, showing no measurable changes in the $E_{11}$ fluorescence peak.

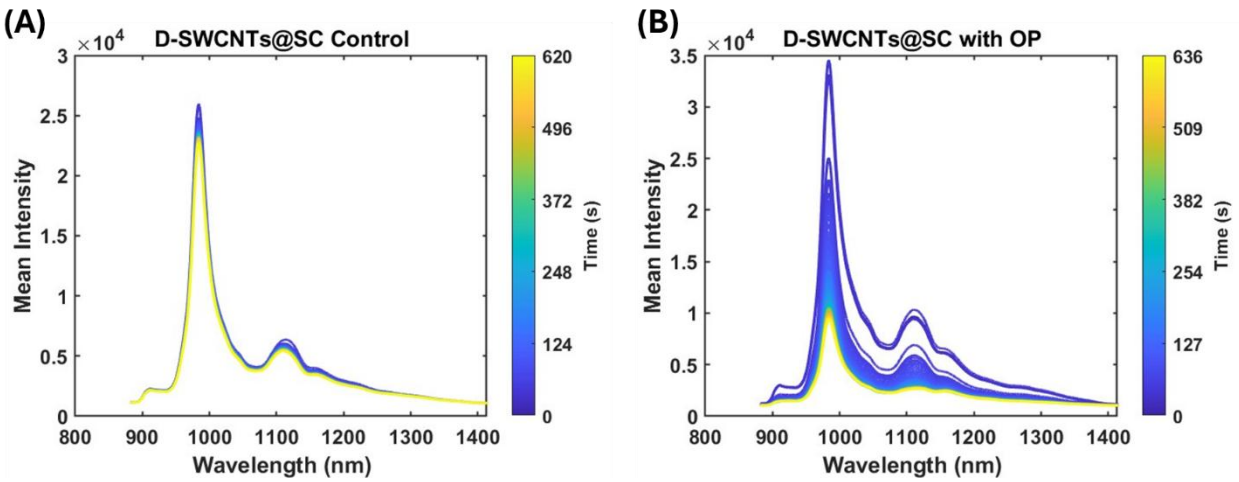


**Figure S5.** Real-time full fluorescence spectra of D-SWCNTs@SC ($E_{11}$>$E_{11}^*$). **(A)** Control measurement following water addition, showing stable fluorescence spectra over time with minimal fluctuations. **(B)** Fluorescence spectra following OP addition, showing a rapid and stable decrease in the $E_{11}$ peak intensity alongside the full spectral profile. Color bars indicate measurement time (s).

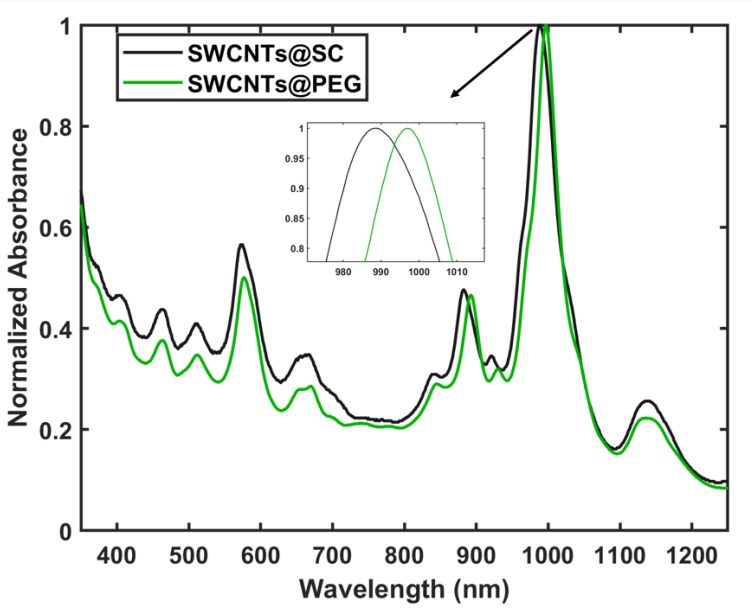


**Figure S6.** UV-Vis-NIR absorption spectra of pristine SWCNTs@SC (black curve) and pristine SWCNTs@PEG (green curve). The spectra are normalized to the $E_{11}$ peak, showing the characteristic absorption features of (6,5)-enriched SWCNTs under different dispersion conditions. The inset highlights a redshift in the $E_{11}$ absorption peak position for SWCNTs@PEG compared to SWCNTs@SC, indicating a successful corona exchange.

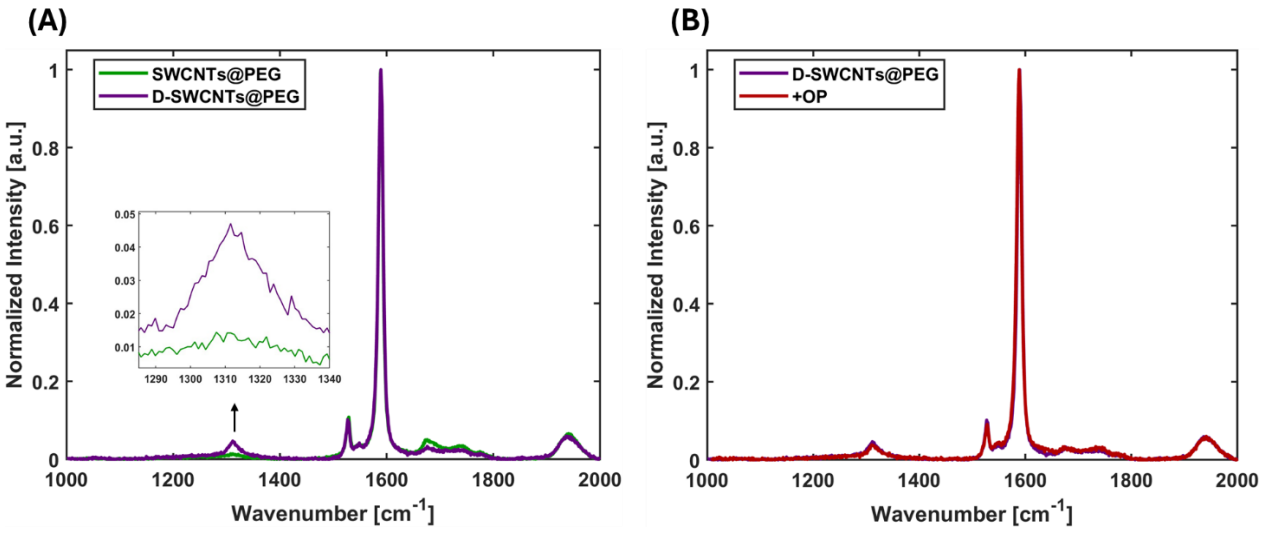


**Figure S7.** Raman spectroscopy. **(A)** Raman spectra of SWCNTs@PEG (green) and D-SWCNTs@PEG (purple) following 5 min UV irradiation. Inset: A distinct D-band is observed in the D-SWCNTs@PEG, signifying the successful introduction of oxygen defects. **(B)** Raman spectra comparing D-SWCNTs@PEG (purple) and D-SWCNTs@PEG after OP treatment (red), showing no apparent difference.

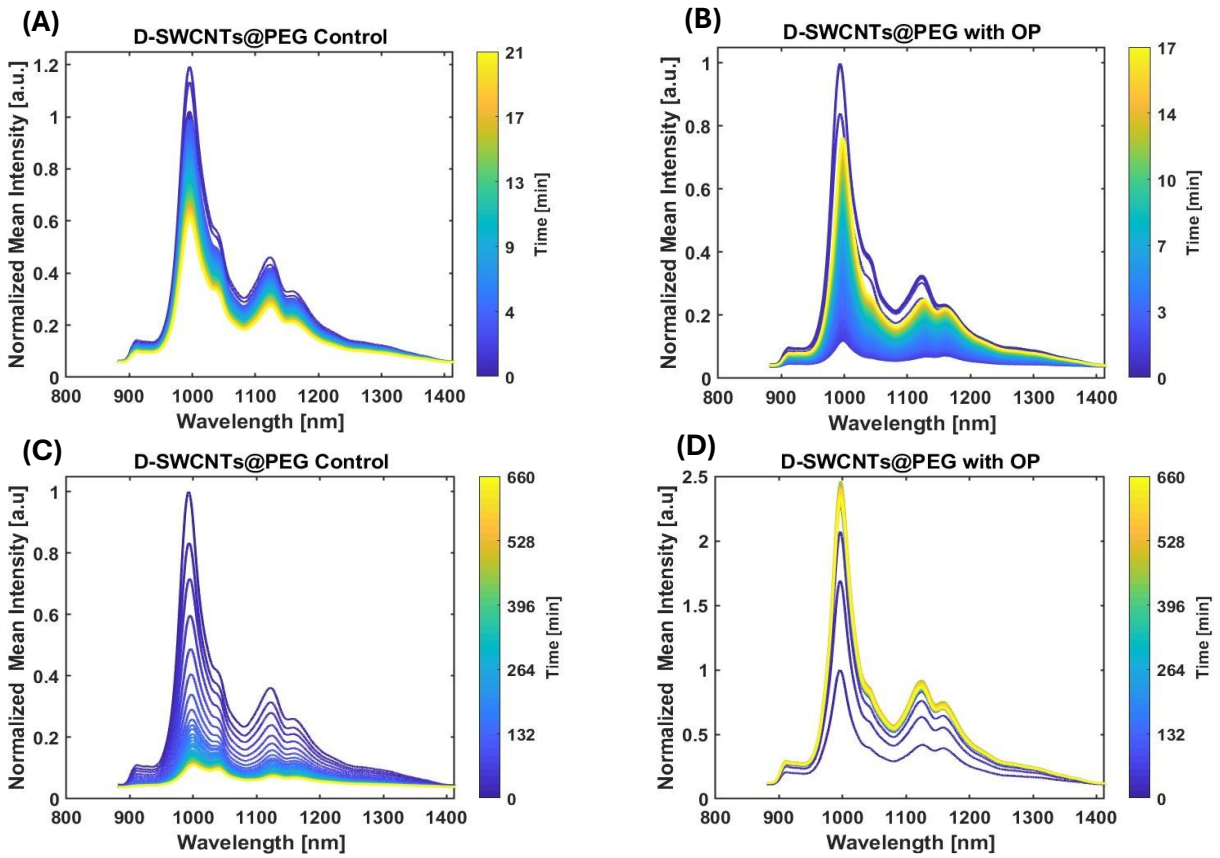


**Figure S8.** Full fluorescence spectra of D-SWCNTs@PEG over time. **(A)** Real-time continuous measurements with 4-second exposure intervals, with water (control) or **(B)** OP added after ~40 seconds, showing the short-term evolution of the fluorescence spectra. **(C)** Extended measurements over several hours with acquisitions every 15 minutes under the same exposure conditions, showing a clear decrease in fluorescence for the control and **(D)** a gradual increase in fluorescence for the OP sample until reaching stable values. All spectra are normalized to the initial fluorescence intensity at the start of the measurement. Color bars indicate measurement time (min).

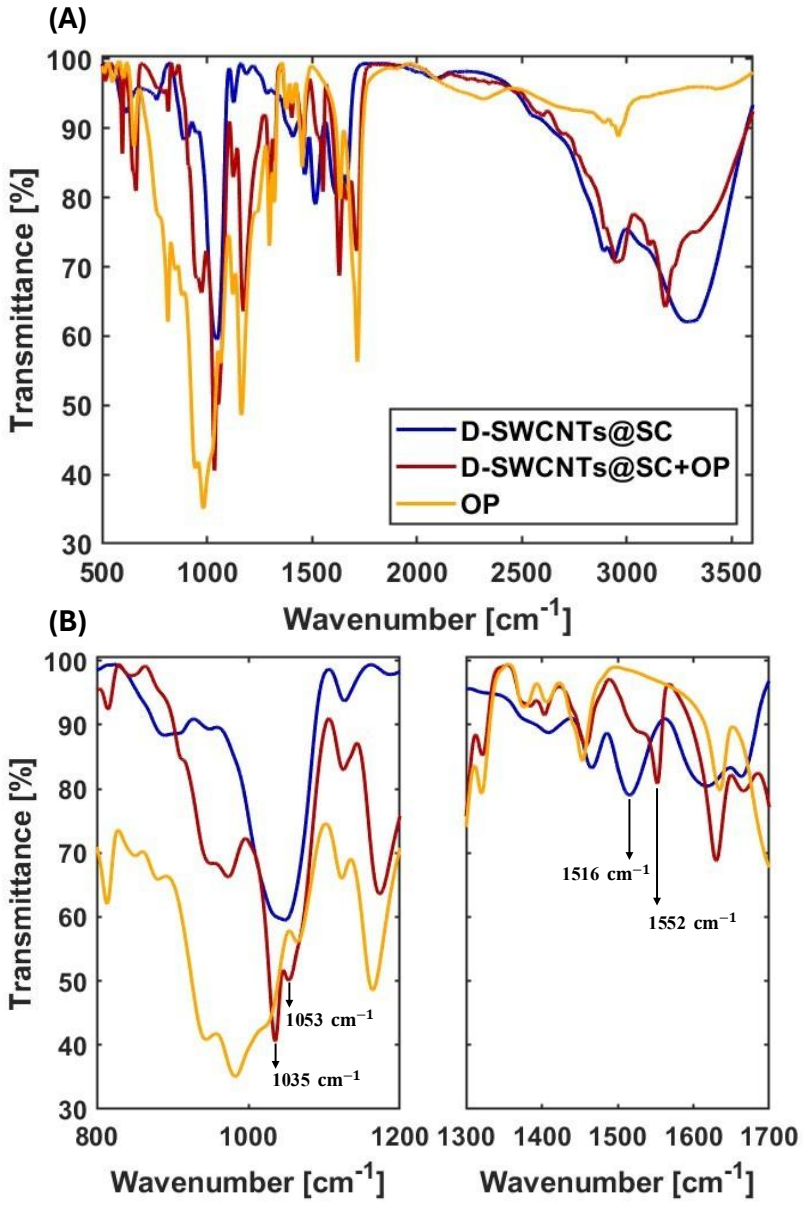


**Figure S9.** FTIR analysis. **(A)** FTIR spectra of D-SWCNTs@SC before (blue) and after (red) treatment with OP, along with the spectrum of OP alone (orange). **(B)** Zoom in on regions of interest.

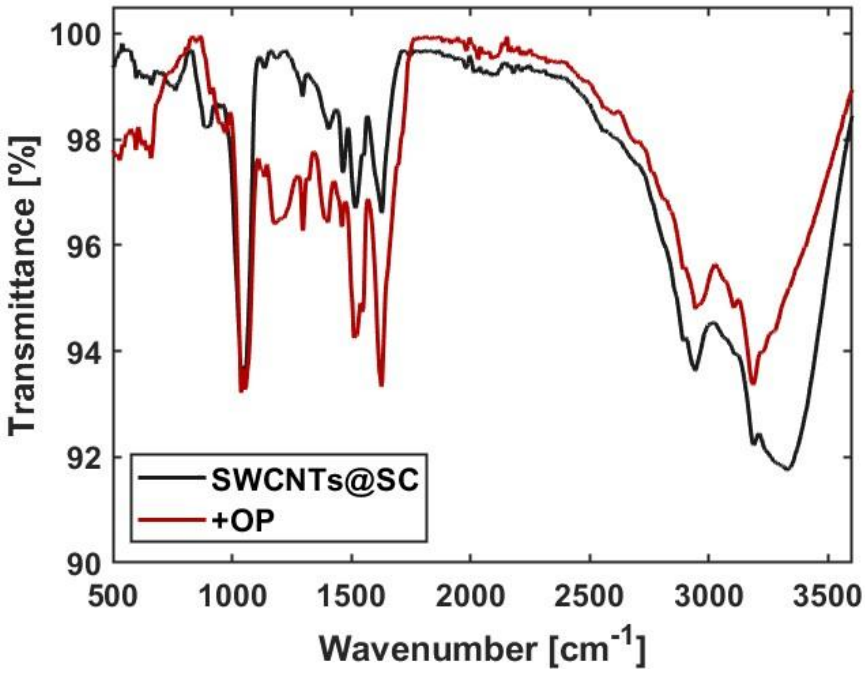


**Figure S10:** FTIR spectra of SWCNTs@SC before (black) and after (red) treatment with OP.

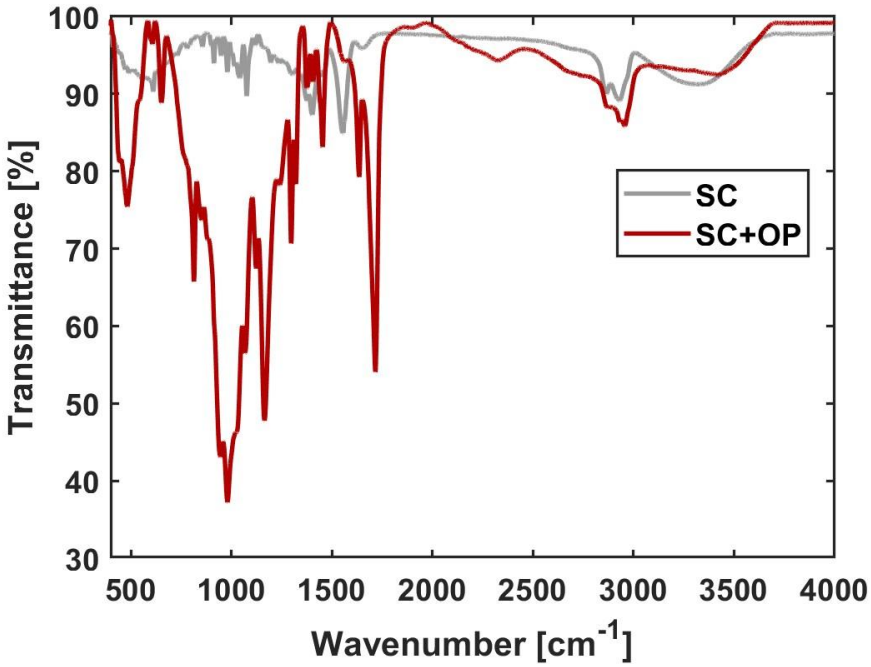


**Figure S11:** FTIR spectra of SC before (grey) and after (red) the addition of OP.

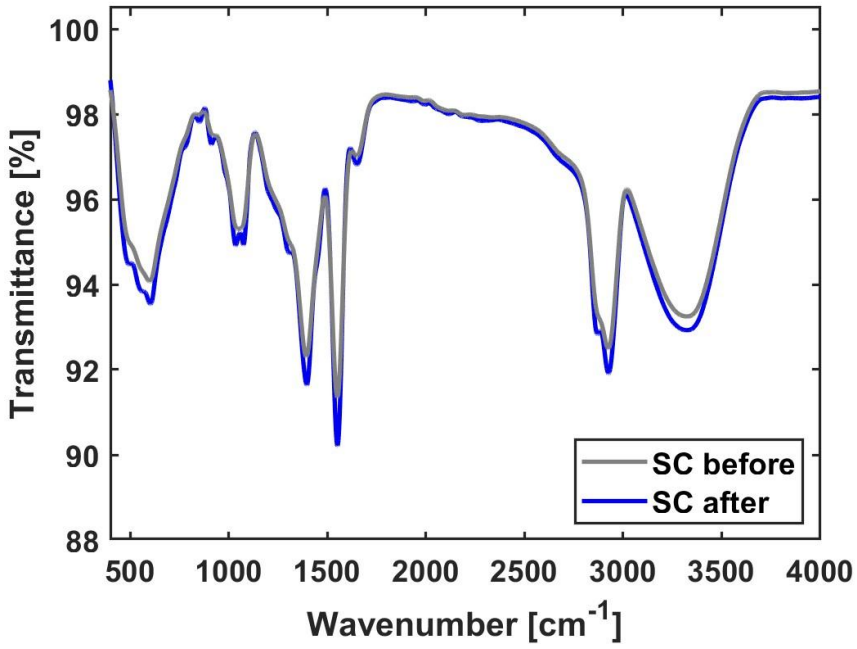


**Figure S12:** FTIR spectra of SC before (grey) and after (blue) treatment with NaClO and UV.

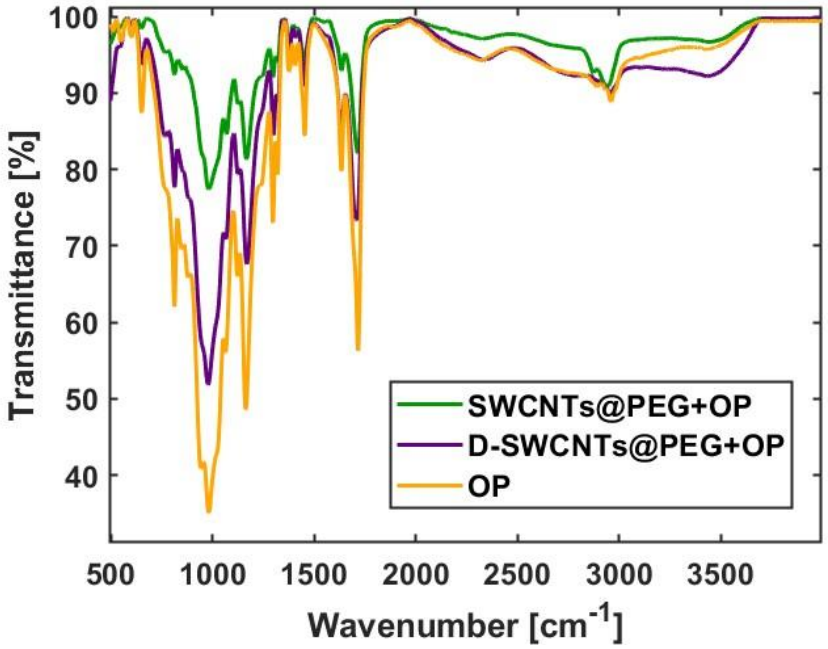


**Figure S13: (A)** FTIR spectra of SWCNTs@PEG (green) and D-SWCNTs@PEG (purple) after treatment with OP, along with the spectrum of OP alone (orange).

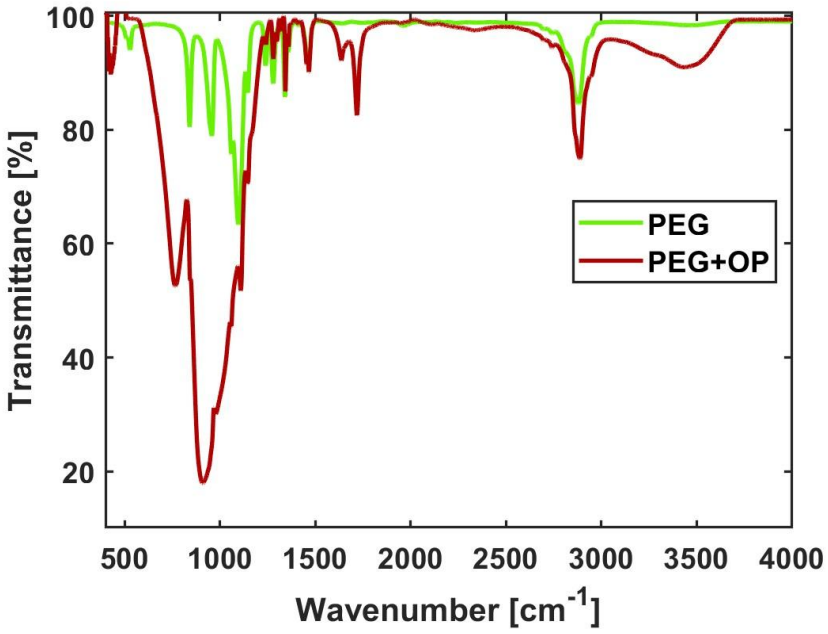


**Figure S14:** FTIR spectra of DSPE-PEG before (light green) and after (red) the addition of OP.

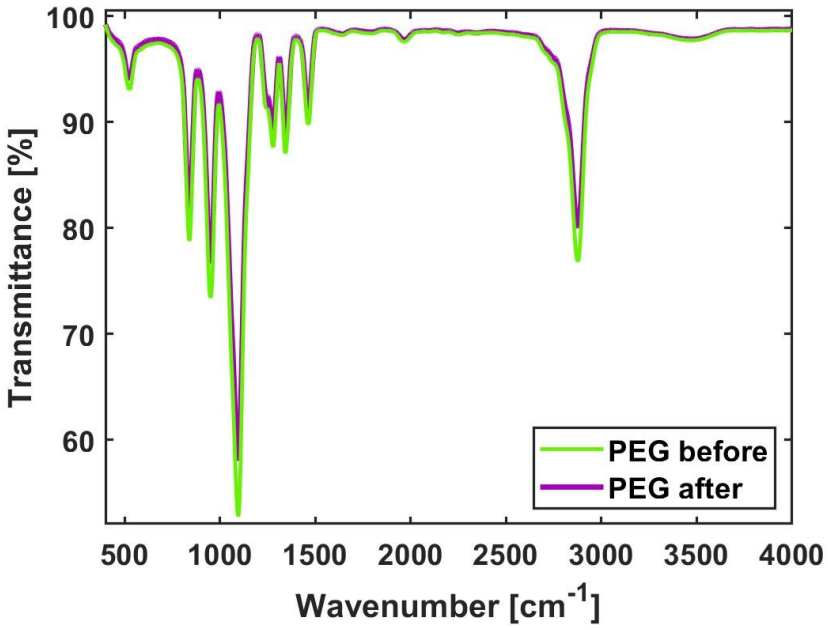


**Figure S15:** FTIR spectra of DSPE-PEG before (light green) and after (purple) treatment with NaClO and UV.

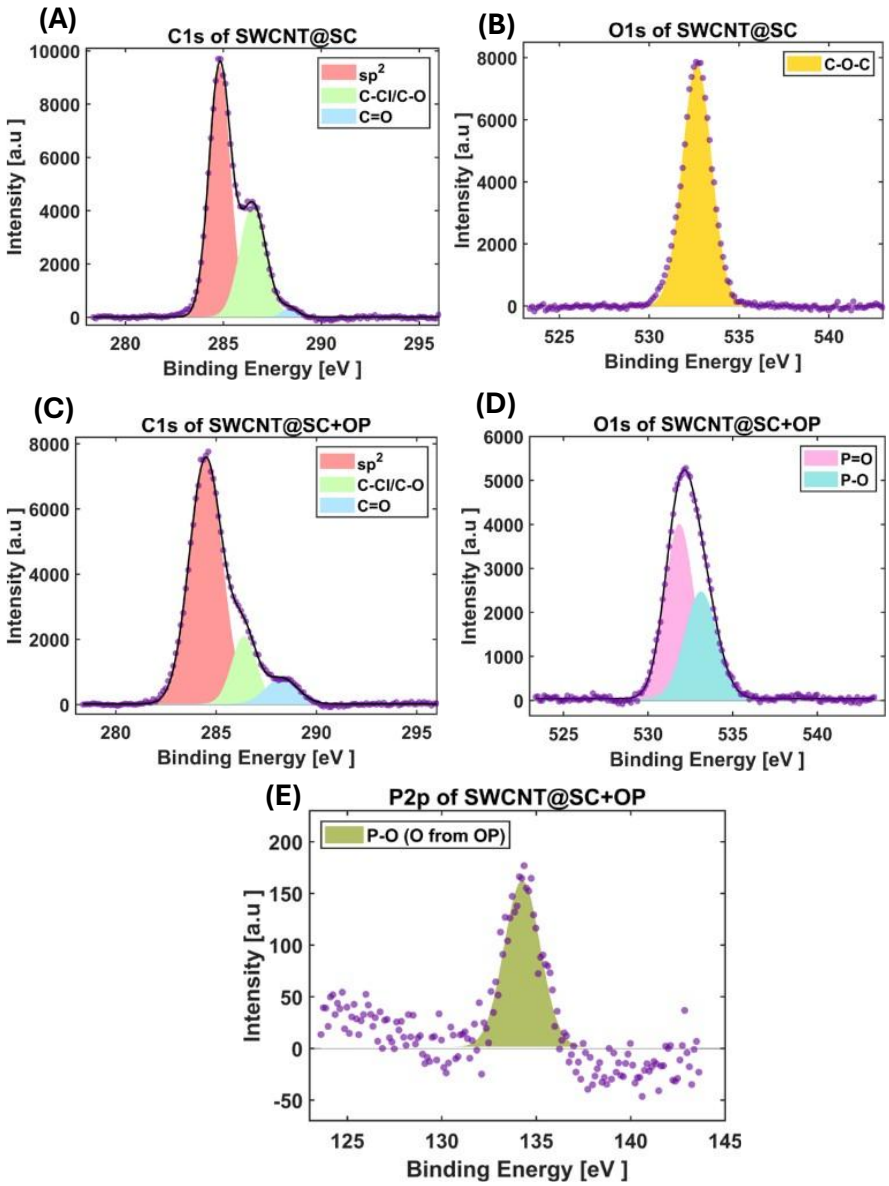


**Figure S16:** High-resolution XPS spectra of SWCNT@SC (A) of C1s and (B) O1s, before the addition of OP. High-resolution XPS spectra of SWCNT@SC (C) of C1s and (D) O1s, after the addition of OP. (E) High-resolution XPS spectra of P2p of SWCNT@SC after the addition of OP. The colored areas represent individual deconvoluted peaks, the black line shows the cumulative fit for multiple peaks, and the purple dots correspond to the experimental data.

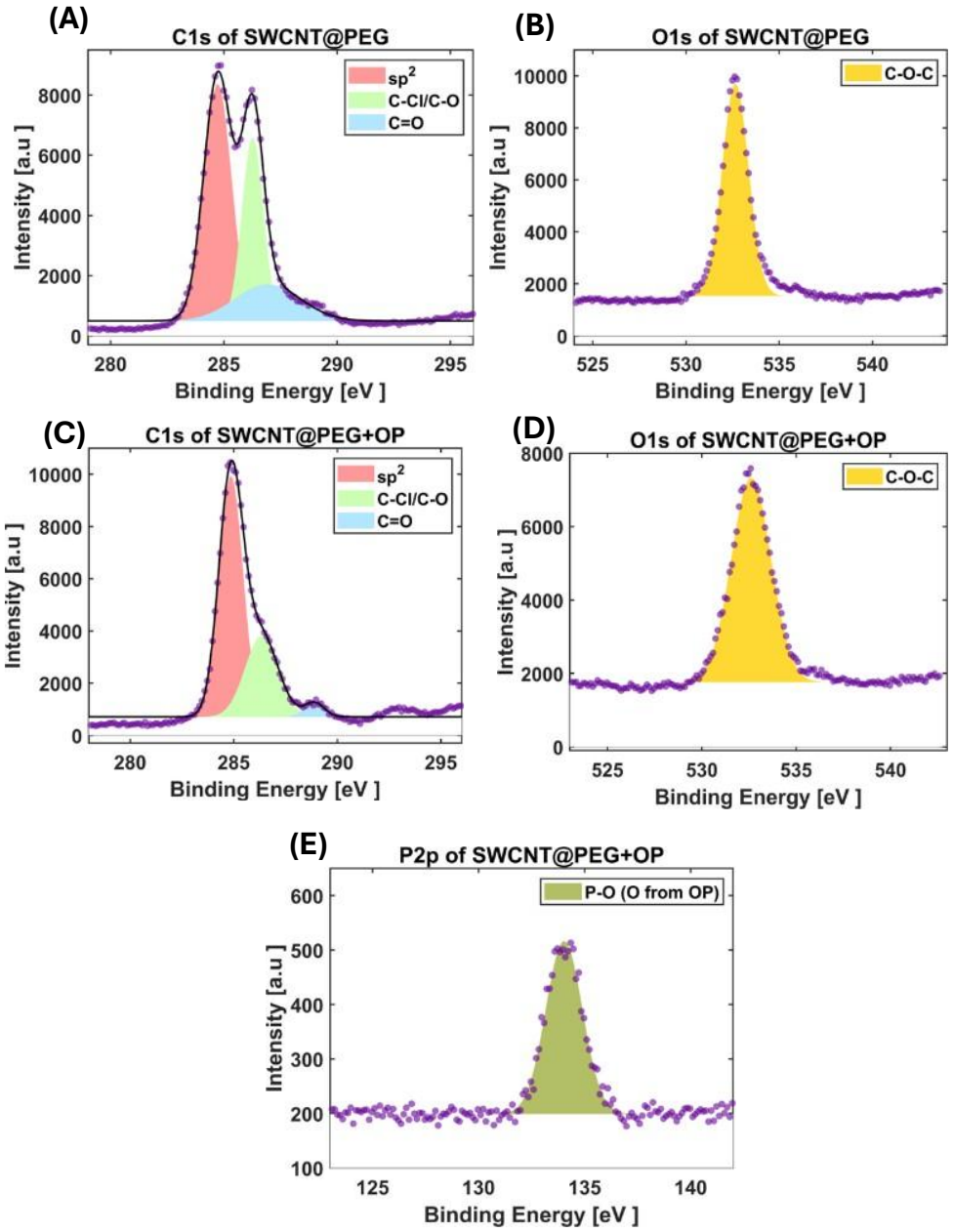


**Figure S17:** High-resolution XPS spectra of SWCNT@PEG **(A)** of C1s and **(B)** O1s, before the addition of OP. High-resolution XPS spectra of SWCNT@PEG **(C)** of C1s and **(D)** O1s, after the addition of OP. **(E)** High-resolution XPS spectra of P2p of SWCNT@PEG after the addition of OP. The colored areas represent individual deconvoluted peaks, the black line shows the cumulative fit for multiple peaks, and the purple dots correspond to the experimental data.